Sedimentary Geology 439 (2022) 106219

Contents lists available at ScienceDirect

Sedimentary Geology

journal homepage: www.elsevier.com/locate/sedgeo

Seismites in Miocene gypsum microbialites: Multiproxy tools for paleoenvironmental reconstruction of saline lakes

M. Esther Sanz-Montero [a,*], J. Pablo Rodríguez-Aranda [b]

[a] Dpto. Mineralogía y Petrología, Fac. Geológicas, Univ. Complutense, C/ José Antonio Nováis, 2, 28040 Madrid, Spain
[b] IES Camilo José Cela, Av. Monte, 14, 28223 Pozuelo de Alarcón, Madrid, Spain

ARTICLE INFO

Article history:
Received 8 June 2022
Received in revised form 25 July 2022
Accepted 26 July 2022
Available online 1 August 2022

Editor: Dr. Brian Jones

Keywords:
Gypsum microbialites
Saline lake
SSDSs
MISS
Duero basin
Madrid basin

ABSTRACT

This work provides the first evidence of seismites within Miocene gypsum microbialites deposited in inland lakes. Seismites are observed on good quality outcrops in two separated successions of the Madrid and Duero basins (central Spain) that are sited nearby strike-slip faults. The successions consist of sandy gypsum facies interbedded with gypsiferous mudstone and marlstone. The association of microbial induced sedimentary structures (MISS) with mineralogical biosignatures such as intrasediment-grown lenticular gypsum, dolomite with inner biomolds and other biological induced minerals, supports that gypsum beds represent microbialites. Gypsum microbialites are characterized by parallel-lamination, cross-bedding and laminated leveling structures. The rapid mineralization of the microbial mats and biostabilization processes may play a role in the preservation of the depositional structures in sulfates. In addition to MISS, several categories of large-scale soft-sediment deformation structures (SSDSs) reflecting ductile and brittle behavior repeat vertically through the successions. These are classified as load casts, pillows, dish structures, convolute bedding and lamination, plastic intrusions, fluid escape tubes, mud/sand volcanoes, Neptunian dikes and fractures. The deformation structures in crystalline sediments are interpreted to be caused by seismic shocks of magnitude over 5 related with syndepositional fault movements. Micromorphological analysis of gypsum beds reveals distinctive features such as cracked crystals, oriented crystals filling dikes and horizontal microstylolites that also indicate seismic shocks. Comparison between the two basins shows some differences in the type and vertical distribution of structures, and this suggests that earthquakes were less frequent and of higher magnitude in the Madrid Basin. The results confirm that microbial gypsum deposits have both high susceptibility to earthquakes and high potential to preserve a wide range of information of the sedimentary environment, including paleoecology, paleogeochemistry, paleohydrodynamics, and seismogenic behavior of microbial sediments and faults.

1. Introduction

Seismites are layers characterized by abundant seismically triggered soft-sediment deformation structures (SSDSs) (Seilacher, 1969) over long distance (van Loon et al., 2016). Some types of brittle deformation may also be classified as seismites (Montenat et al., 2007). Soft-sediment deformation structures, particularly seismites, are strongly influenced by the sedimentary environment since they usually occur at surface or close to it, where sedimentary processes physically interact with unconsolidated sediments (Allen, 1982; Moretti et al., 2016). Accordingly, seismites are useful tools for reconstructing paleoenvironments and paleoseismicity in sedimentary basins. SSDSs have been most frequently found in siliciclastic deposits comprised of fine-grained sediments with contrasted granulometry since these are the most earthquake-prone sediments (Montenat et al., 2007).

Evaporites, including gypsum rocks, show abundant hydroplastic deformations (SSDSs), commonly interpreted as diagenetic processes caused by intrasediment precipitation, burial and consolidation, or mineral reactions associated to volume change (Warren, 2016). Other SSDSs are related to depositional slopes and resedimentation of gypsum/anhydrite deposits by high-density flows (Vai and Ricci-Lucchi, 1977; Peryt and Kasprzyk, 1992; Peryt and Jasionowski, 1994; Rouchy et al., 1995), which can be interpreted as turbidites produced by seismic shocks (Peryt and Kasprzyk, 1992; Peryt and Jasionowski, 1994). However, sensu stricto seismites (Montenat et al., 2007; Shanmugam, 2016) have been scarcely documented in ancient gypsum–anhydrite rocks (Rossetti and Góes, 2000; Bachmann and Aref, 2005; El Taki and Pratt, 2012). Modern analogs for gypsum seismites are even rarer, apart from descriptions provided by Aref (1998) in Holocene deposits of Egypt.

* Corresponding author.
E-mail address: mesanz@ucm.es (M.E. Sanz-Montero).

https://doi.org/10.1016/j.sedgeo.2022.106219

The scarcity of seismic deformation structures reported in evaporites may be due to the cohesive behavior of the early cemented sediment, the similarity of crystallization structures with deformations caused by seismic shocks, and the pervasive diagenetic processes that obliterate those features (Bachmann and Aref, 2005). This may render evaporite SSDS interpretation difficult, particularly in weathered outcrops.

Exceptionally, clastic gypsum deposits with good preservation of depositional structures, including SSDSs, occur in Miocene lacustrine successions of the Madrid and Duero basins, central Spain (Mediavilla, 1986-1987; Sanz-Montero et al., 1994; Sanz-Montero, 1996; Muñoz et al., 2007). On basis of detailed analyses of undeformed dolomitic rocks overlying the clastic gypsum deposits of the Duero basin, Sanz-Montero et al. (2008) concluded that microbial mats thriving in the lakes mediated the precipitation of dolomite and the associated minerals, resulting in extensive formation of microbialites in shallow lakes. However, the appearance of microbial textures and structures in gypsum rocks may differ from that of carbonates deposited in more diluted conditions (Sanz-Montero et al., 2009). This work aims to study the type of microbial features preserved in gypsum deposited in shallow saline lakes of the Madrid and Duero Basins. The occurrence of modern lacustrine environments where similar microbial deposits are forming in central Spain (Sanz-Montero and Rodríguez-Aranda, 2013; Sanz-Montero et al., 2015; Cabestrero et al., 2018) helps to interpreting microbial features in ancient gypsum rocks (Rouchy and Monty, 2000). In addition, the occurrence of deformation structures in these rocks provides a unique opportunity of investigating the development and preservation of deformation structures in microbial gypsum rocks. Based on the study of the two basins, this research shows the diversity of SSDSs in microbial gypsum deposits and provides criteria to interpret such structures as seismites. Spatial and temporal evolution of seismites in sulfate rocks helps to understanding the seismogenic behavior of both microbial gypsum and faults in environments depleted of siliciclastic deposits.

2. Geologic setting

Sedimentary structures were studied in two 400 km-separated gypsum-bearing successions in the center of the Iberian Peninsula (Figs. 1, 2 and 3). The successions are located in the Madrid and Duero basins that are Cenozoic continental depressions separated by the Central System mountain range (Fig. 1). The Central System is a thick-skin chain with a NE–SW structural trend that formed during the Alpine orogeny (Calvo et al., 1996). The Alpine deformation was accomplished during the Oligocene–Miocene under a NW–SE to NNW–SSE shortening (De Vicente et al., 2011). The Variscan basement structures of the basins reactivated and worked as strike-slip faults. Such faults acted as lateral ramps of the thrust structures that lift the basin margins during the lower–middle Miocene (De Vicente et al., 2011; De Vicente and Muñoz-Martín, 2013). Each of the study-zones is close to these lateral ramps in the Madrid and Duero basins (Fig. 1).

2.1. Madrid Basin

The Miocene record of the Madrid Basin is divided into three main flat-lying lithostratigraphical units: Lower, Intermediate and Upper (Calvo et al., 1996), each separated by discontinuities related to major tectonic activity in the margins (Fig. 1). The studied sedimentary successions form the basal part of the Intermediate Unit (Burdigalian) that lies paraconformably on the deposits of the Lower Unit (Rodríguez-Aranda et al., 2002). The general sedimentary framework for the Intermediate Unit is established as an alluvial fan-saline lake complex characteristic of a hydrologically closed basin (Calvo et al., 1996), where the lacustrine carbonate and gypsum interfinger with mudstones in marginal areas of the lakes. The up to 10 m thick studied profiles are located in a radius of 10 km around the town of Huerta de Valdecarábanos (HV), nearby a NW–SE right-lateral strike-slip fault related with the south margin of the basin (Toledo Mountains) (Fig. 1). The profiles consist of gypsum (clastic and microbialites), gysiferous mudstone, and dolomite layers (Figs. 2, 4A, 5A, C). The succession deposited in saline mudflat-shallow lake environments affected by storm events (Sanz-Montero et al., 1994; Sanz-Montero, 1996).

2.2. Duero Basin

Seven main lithostratigraphic units have been distinguished in the sedimentary record of the Duero Basin (Armenteros et al., 2002)

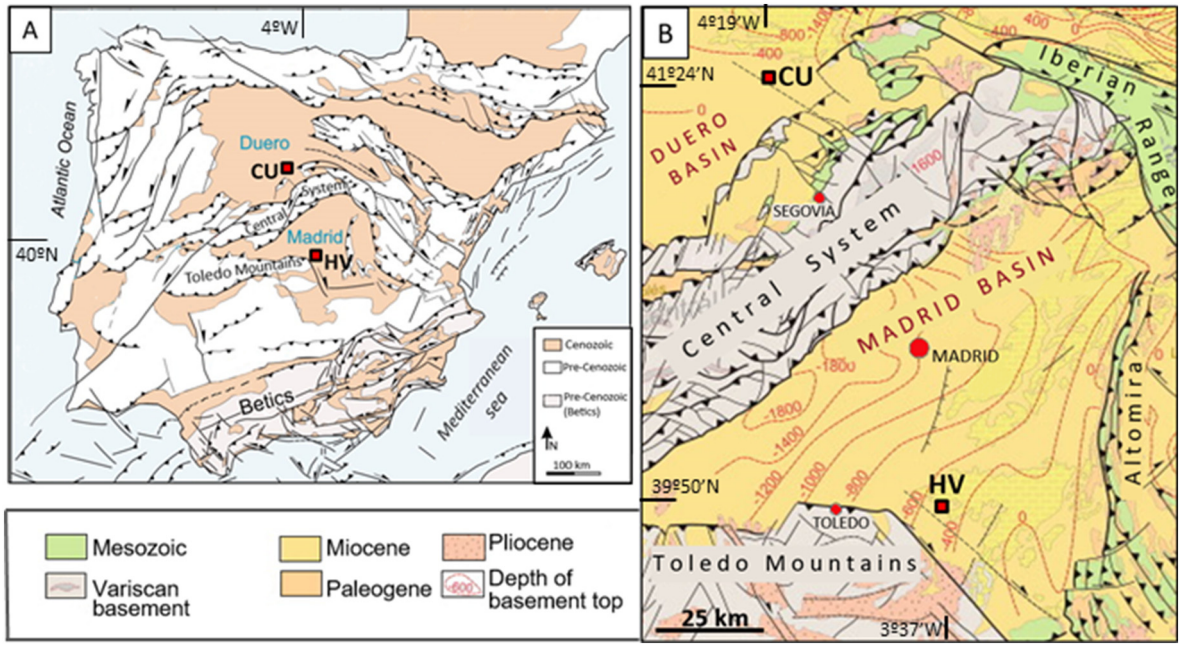

Fig. 1. Location of the study zones showing the relationships with the main regional fractures. Modified from De Vicente and Muñoz-Martín (2013). A) Tectonic map of the Iberian Peninsula including the main Cenozoic basins and ranges. B) Map of the Madrid Basin and Southern part of the Duero Basin. Note the close location of the study zones to NW–SE strike-slip faults in the basin basement. CU: Cuéllar area, HV: Huerta de Valdecarábanos area.

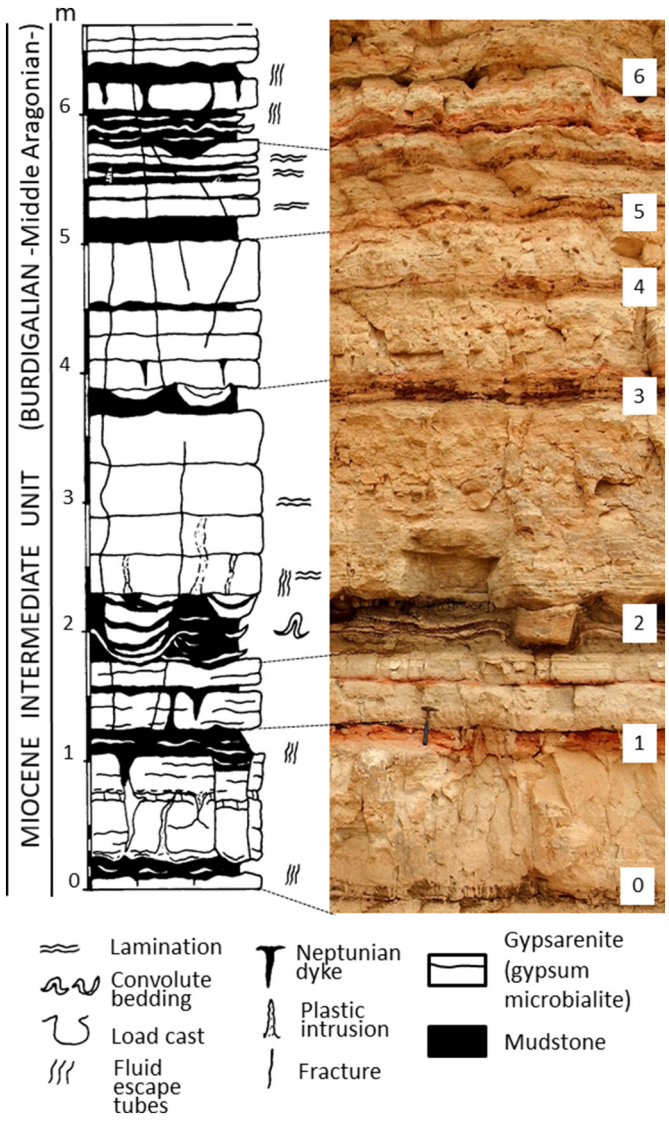

Fig. 2. Stratigraphic log of Huerta de Valdecarábanos including seismites in the lowermost interval of the Miocene Intermediate Unit (Burdigalian). Some representative beds are numbered in the photo.

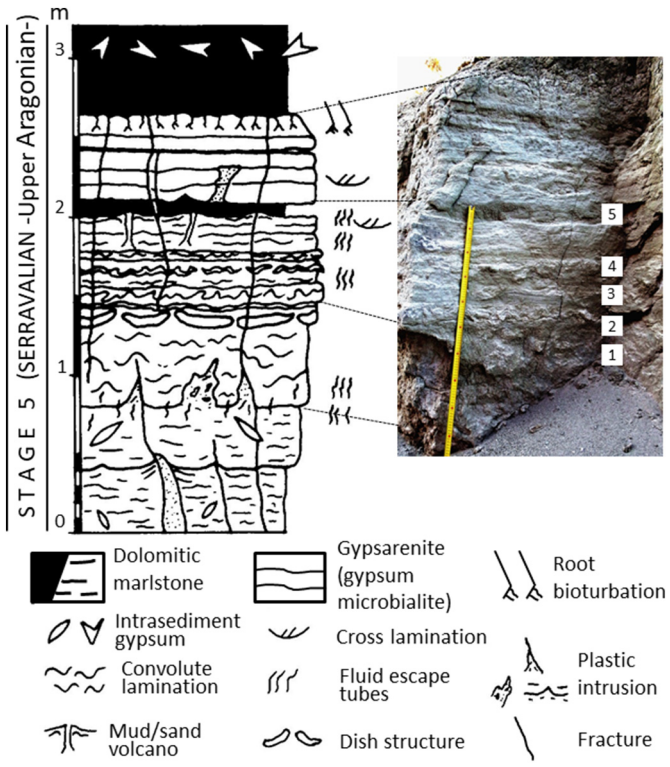

Fig. 3. Stratigraphic log of Cuéllar showing deformation structures in middle Miocene deposits (Serravalian). Some representative layers are numbered in the photo.

(Fig. 1A). The present study is focused on the 5 m thick basal interval of the up to 80 m thick stratigraphical section outcropping in the Cuéllar (CU) area (Sanz-Montero et al., 2008). The gypsum-bearing outcrops (Fig. 1B) are sited along a 23 km band in the vicinity of a NW–SE left-lateral strike-slip fault (Fig. 1). Gypsum beds comprise the uppermost middle Miocene succession in the area, which is equivalent to the sedimentary *stage 5* of Armenteros et al. (2002). Deposits of stage 5 lie horizontally on a disconformity that resulted from the uplift of the Central System. During this stage marginal alluvial fans grew and fed large fluvial systems that progressively receded and gave way to gypsiferous shallow saline lakes in the Serravalian (Armenteros, 1991; Armenteros et al., 2002; Sanz-Montero et al., 2008). The study successions consist of gypsum interbedded with gypsiferous mudstone and marlstone facies (Figs. 3, 4B, C, 5B, D).

3. Materials and methods

Field work involved delimitation and selection of well-exposed outcrops around the villages of Cuéllar (41°24′10″N; 4°19′12″W) and Huerta de Valdecarábanos (39°49′49.33″N; 3°37′7.03″W) located in the Duero and Madrid Basins, respectively. Selected outcrops, mainly inactive gypsum quarries and underground mines, were logged and sampled after detailed examination of sedimentary and deformation structures. Besides, geological and topographical maps as well as satellite and aerial photos have been observed to identify fault traces. The mineralogy of samples was determined by X-ray diffraction (XRD). Random powder XRD analyses were carried out for total mineralogy and oriented mounts for clay determinations using a Philips PW-1710 diffractometer and Bruker D8 Advance diffractometer under monochromatic Cu Kα radiation operating at 40 kV and 30 mA. Optical and fluorescence examinations of standard thin-sections stained for carbonates were performed with a white light source and a green-ultraviolet filter, respectively. Generally, soft samples were dehydrated by lyophilization, embedded and impregnated with Epofix resin in order to prepare thin sections. High-resolution textural and morphometric analyses were carried out using secondary electron microscopic (SEM) images and backscattered (BSE) micrographs with elemental composition. They were obtained using SEM-EDAX of a JEOL JSM-6400 operating at 20 kV and equipped with an energy dispersive X-ray microanalyzer.

4. Results

4.1. Sedimentary successions and paleoenvironment

The studied successions of Duero (CU) and Madrid (HV) basins comprise gypsum microbialites interbedded with gypsiferous mudstone and marlstone that can be traceable laterally for several tens of meters and several hundred meters, respectively (Figs. 2–5). In CU, successions are overlaid by gently dipping marlstone beds that laterally may disappear (Fig. 4B). In HV, gypsiferous beds pass sharply into massive mudstone.

Distinctively, the sequences in both areas show SSDSs and synsedimentary microfractures. Mudstone and marlstone deposits contain variable amounts of carbonate, mainly dolomite. In CU, green dolomitic marlstones including lenticular gypsum (mm–cm in diameter) occur as 2–50 cm thick tabular beds (Figs. 3, 4C, 5B, 10C,

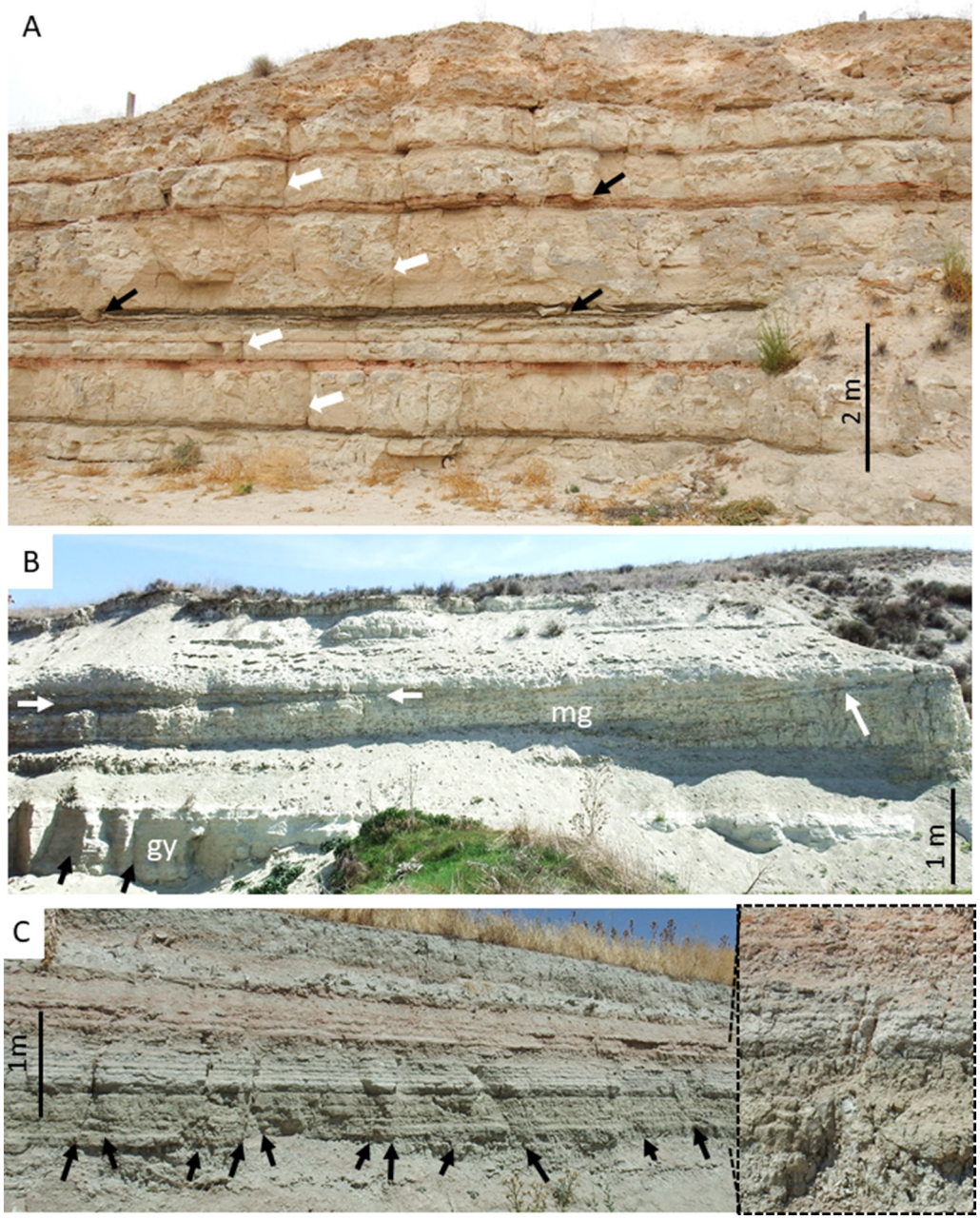

Fig. 4. A) Outcrop showing tabular gypsum microbialites and interbedded mudstone beds in an inactive quarry at Huerta de Valdecarábanos. Some SSDSs are arrowed in black and fractures in white. B) View of a gypsum outcrop in Cuéllar. A gypsum microbialite bed (gy) shows subvertical joints (arrowed). Beds comprising mudstone/marlstone with intrasediment-grown gypsum macrocrystals (mg) dip to the left (inclined arrow), overlaid by a sediment wedge that disappears to the right (horizontal arrows). C) Synsedimentary fractures (arrowed) in stacked gypsarenite beds, Cuéllar area. The inset shows a plastic intrusion associated to a fracture.

E, F). It is remarkable the absence of quartz and feldspars grains in these beds. The mineralogy of phyllosilicates consists of illite (30–60 %), smectite (10–40 %), palygorskite (10–35 %), sepiolite (0–15 %) and kaolinite (<10 %). In HV, these facies form greenish or reddish tabular beds from 5 to 100 cm in thickness and several hundred meters of lateral continuity (Figs. 2, 4A, 8, 9). The facies comprise intrasediment-grown gypsum crystals (up to 50 % by volume) that are 0.5 to 3 mm in size and show subeuhedral and hemipyramidal shapes. The phyllosilicates include illite (50–90 %), palygorskite (0–25 %), smectite (0–20 %) and kaolinite (5–10 %). Minor quartz and dolomite are also present (<10 %).

The general sedimentary model for the successions is established as an alluvial fan-saline lake complex characteristic of a hydrologically-closed basin (Fig. 1). Mudstone and marlstone lithologies represent deposition in a saline lake margin during dilution episodes (Sanz-Montero, 1996; Sanz-Montero et al., 2008). In modern gypsum depositing lakes, illite and smectites are interpreted to be predominantly derived from basin margins, whereas palygorskite, sepiolite and some smectites are observed to form in situ, as well as gypsum and carbonates (Del Buey et al., 2018, 2021).

4.2. Gypsum microbialites

4.2.1. Description

The term microbialites is used here in the sense of Grey and Awramik (2020), i.e., embracing both the lithified microbial mats and the microbial induced sedimentary structures, MISS (Noffke et al., 2001; Noffke, 2010). The average thickness of microbialites ranges

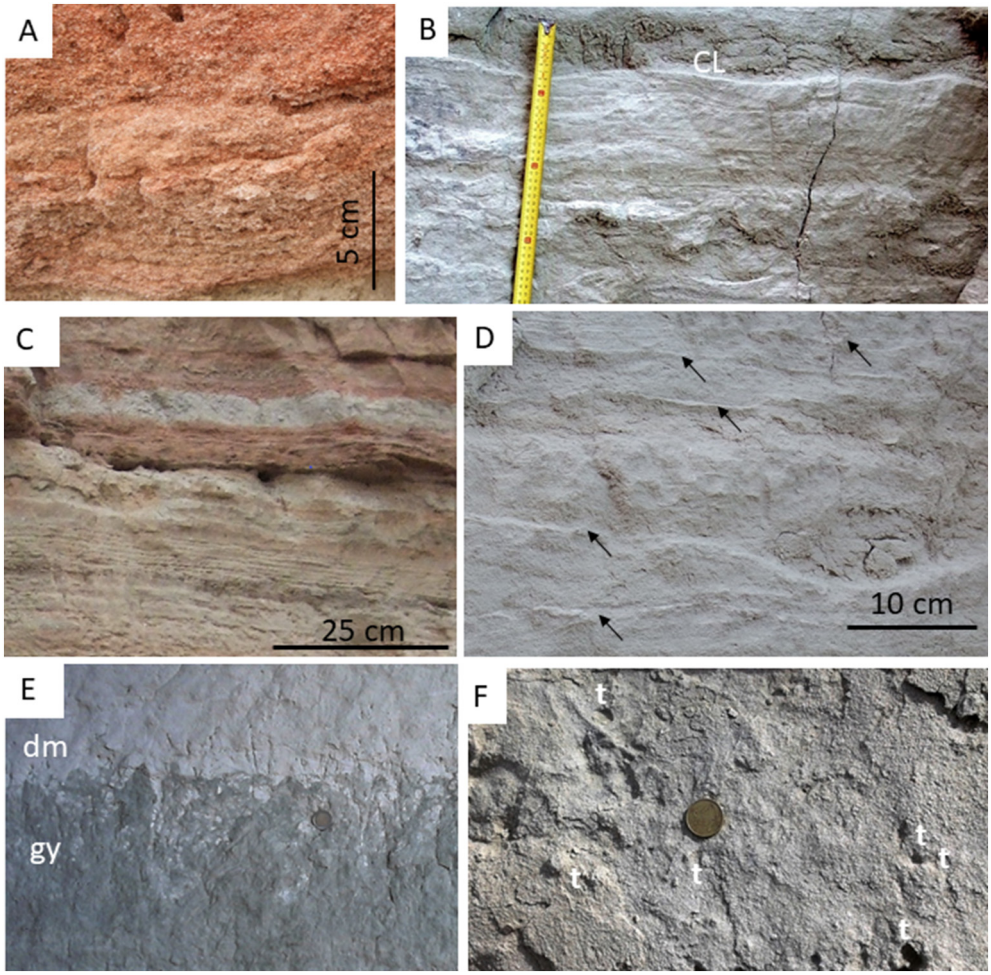

Fig. 5. Field views of gypsum microbialites in Huerta de Valdecarábanos (A and C) and in Cuéllar areas (remaining pictures). A) Coarse gypsarenite with cross lamination. B) Gypsum bed showing undulate lamination and wave ripples. C) Cross section of a laminated gypsum microbialite, where lamination is defined by variable amounts of dolomite. D) Gypsarenite beds that intercalate thin dolomite laminae (arrowed), showing cross-bedding. Notice that carbonate laminae level the topography of the rippled surface. E) Irregular boundary between a gypsarenite (gy) and a dolomitic marlstone (dm) delimited by small SSDSs: flames, fluid scape tubes, drops and drags. Coin for scale = 23 mm. F) Top view of a gypsum microbialite bed showing a smooth and coherent surface where mat fragments along with fluid escape holes and tubes (t) are well preserved. Coin diameter = 24 mm.

between 5 and 20 cm in CU (Figs. 3, 4B, C) and between 10 and 50 cm in HV (Figs. 2, 4A). The microbialites comprise gypsum (50–85 %), commonly showing clastic texture, dolomite (5–40 %), phyllosilicates (10–30 %) and locally ankerite (up to 8 %). SEM analysis also detects minor although pervasive celestite crystals (Fig. 7B).

Microbialites are characterized by laterally extensive planar to undulated laminated structure, vaguely defined ripple marks and cross-bedding. Planar and continuous laminae of carbonates commonly cover the upper planes of the beds, forming laminated leveling structures (Figs. 5D, F, 10C). Besides, mat clasts occur on the top of some beds (Fig. 5F). Erosive bases are seldom observed (Figs. 2, 3).

In thin sections, the laminated gypsum encompasses mm lamina of carbonate and intrasediment-grown gypsum crystals. The latter commonly show a matrix-supported fabric, with gypsum crystals lying horizontally and embedded by a dark matrix (Fig. 6A). Under fluorescence microscopy the matrix fluoresces, indicating that it contains carbonaceous compounds in addition to fine sized dolomite, minor phyllosilicates (mainly sepiolite) and celestite (Figs. 6A, B, 7B–D). SEM analysis reveals that the carbonaceous substances form smooth films on which dolomite and celestite are nucleated as isolated crystals. Pervasively, dolomite crystals contain an inner, spheroidal hole (Fig. 7D). Gypsum crystals are predominantly lenticular, but hemipyramidal euhedral to rounded shapes are also observed (Figs. 6, 7A). Monocrystalline gypsum grains are far more abundant than twinned crystals and aggregates. Clear and idiomorphic gypsum overgrowths formed in repeated episodes of cementation commonly cover in optical continuity the original nucleus, which are dark due to the matrix inclusions (Fig. 6A–D). The surfaces of the crystals show heavy pitting corrosion filled by the components of the matrix (Fig. 6F).

Laminated gypsum occurs associated to gypsum beds showing vaguely defined ripple marks and cross-bedding. These deposits are gypsarenite as they comprise fine to coarse sand sized crystals (0.064–2 mm) in the Madrid basin (Figs. 4A, 5A, C, 6C,D, 7A), and fine to medium sized grains (0.064–0.5 mm) in the Duero basin (Figs. 4B, C, 5B, D, F, 6A, B). In thin sections the gypsarenites are made up of abraded gypsum grains as well as intraclasts of dolomite and mudstone (Fig. 6A, E). The formation of synsedimentary overgrowths of gypsum, infilling the intergranular spaces, results in a crystal-supported fabric that obliterates the abrasion features and very often the crossbedding (Figs. 6C, 7A). Under a microscope, ripple crests consist of inclined laminae of gypsum alternating with thin laminae of carbonates, while the ripple throughs are commonly filled with horizontal laminae of gypsum and carbonate. The tops of successive ripple crests appear outlined by carbonate drapes that overprint the topography (Figs. 5D, 6B).

4.2.2. Interpretation

The occurrence of ancient gypsum deposits showing wavy to planar laminites and columnar buildups, has been reported in different locations. These deposits are named mineralized or gypsified microbial mats; or, more generally, gypsum microbialites (Rouchy and Monty,

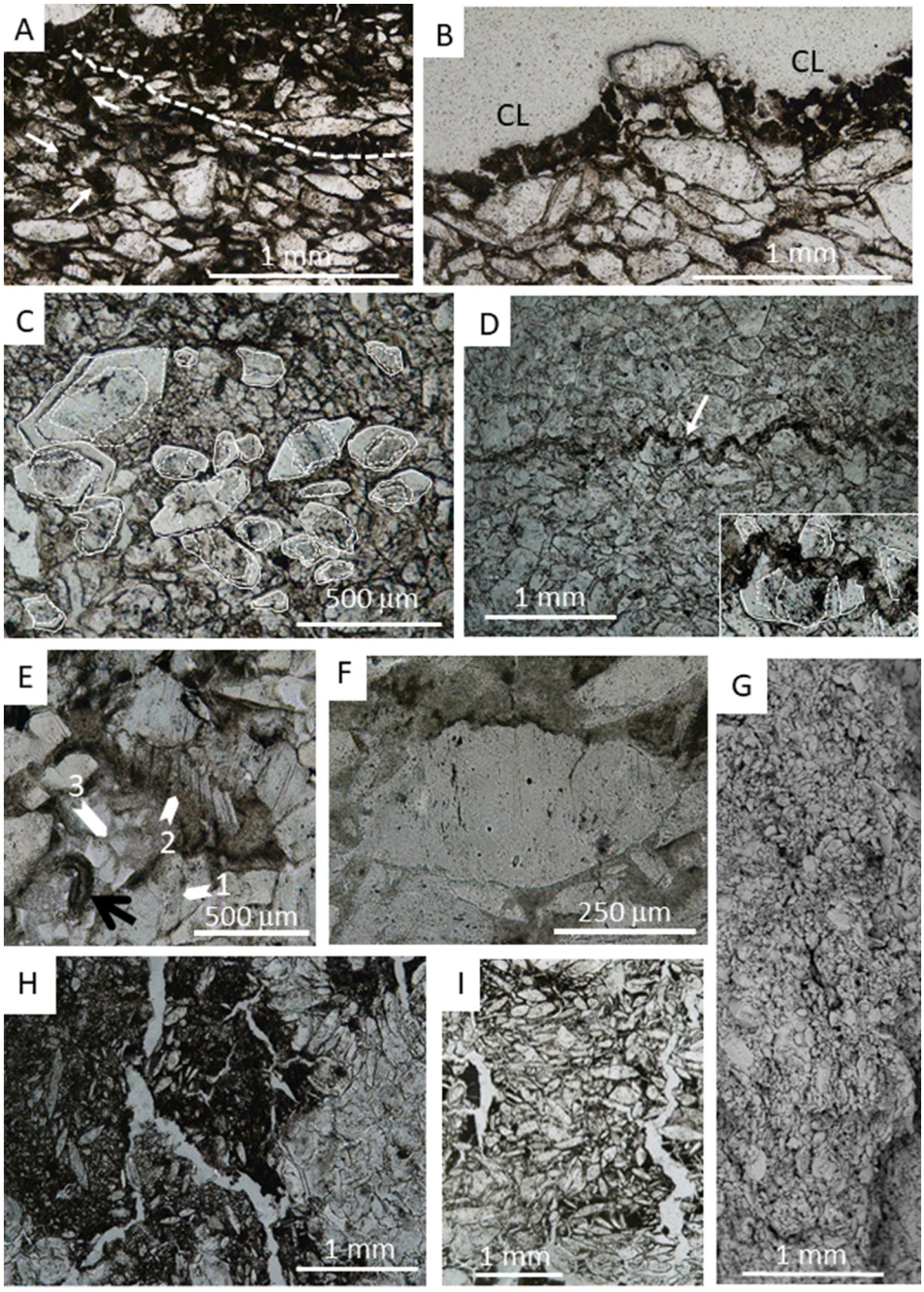

Fig. 6. Light microscope microphotographs and SEM image (G) of gypsum microbialites showing rounded to lenticular gypsum. Crystals often exhibit epitaxial overgrowths and inclusions. C, D and G are from HV area, the rest from CU. A) Detail of ripples consisting of inclined gypsum lenses and mud intraclasts (arrowed). A ripple through (dashed line) is filled with gypsum and carbonate lying horizontally. Notice that the carbonate content increases upwards as the size of gypsum crystals decreases. B) Dolomicrite lamina (CL) covering a gypsarenite layer. C) Microfabric of gypsarenite showing crystals with dark nucleus and successive overgrowths (outlined). D) Serrated microstylolite in a gypsarenite marked by an insoluble residue of dolomite. A detail of crystal dissolution (arrowed) is magnified in the inset. E) Crystals of gypsum broken preferently along (010) main exfoliation plane (arrowed). Three stages of breakage are numbered: (1) initial breakage, (2) displaced fragments, (3) separated fragments. A fragment of laminated carbonate is arrowed in black. F) Gypsum crystal showing pitting and corrosion. G) SEM image of the infilling of a Neptunian dike by gypsum crystals that are arranged vertically. H), I) Horizontal and vertical sections of a mud/sand volcano structure showing the ejected masses and a net of fluid scape pipes.

2000; Babel, 2004; Allwood et al., 2013; Sanz-Montero et al., 2013). Similar laminated gypsum deposits are also forming in modern hypersaline settings where microbial mats develop (Ortí et al., 1984; Rouchy and Monty, 2000; Sanz-Montero et al., 2013; Cabestrero and Sanz-Montero, 2018; Cabestrero et al., 2018; Aref et al., 2020; Del Buey et al., 2021). Observations in modern saline lakes of central Spain have revealed that subaqueous precipitation of gypsum crystals does not proceed spontaneously in the water. Instead, fine crystals of lenticular gypsum nucleate within the microbial mats together with carbonates, phyllosilicates and celestite, forming vaguely laminated to massive microbialite deposits (Sanz-Montero et al., 2013; Cabestrero and Sanz-Montero, 2018; Cabestrero et al., 2018; Del Buey et al., 2021). The intrasediment growth of gypsum and associated minerals is favored by the EPS matrix ability of the microbial mats of sequestering large amounts of S, Si, Ca and Mg, among others, from the overlying water (Del Buey et al., 2021). Unlike other sulfates, the lenticular gypsum crystallizes distinctively within mats in the submerged areas of the lake (Del Buey et al., 2021). As Miocene crystals, modern gypsum shows distinctive overgrowth and corroded zones reflecting episodic stages of growth and dissolution controlled by the seasonal variations in the

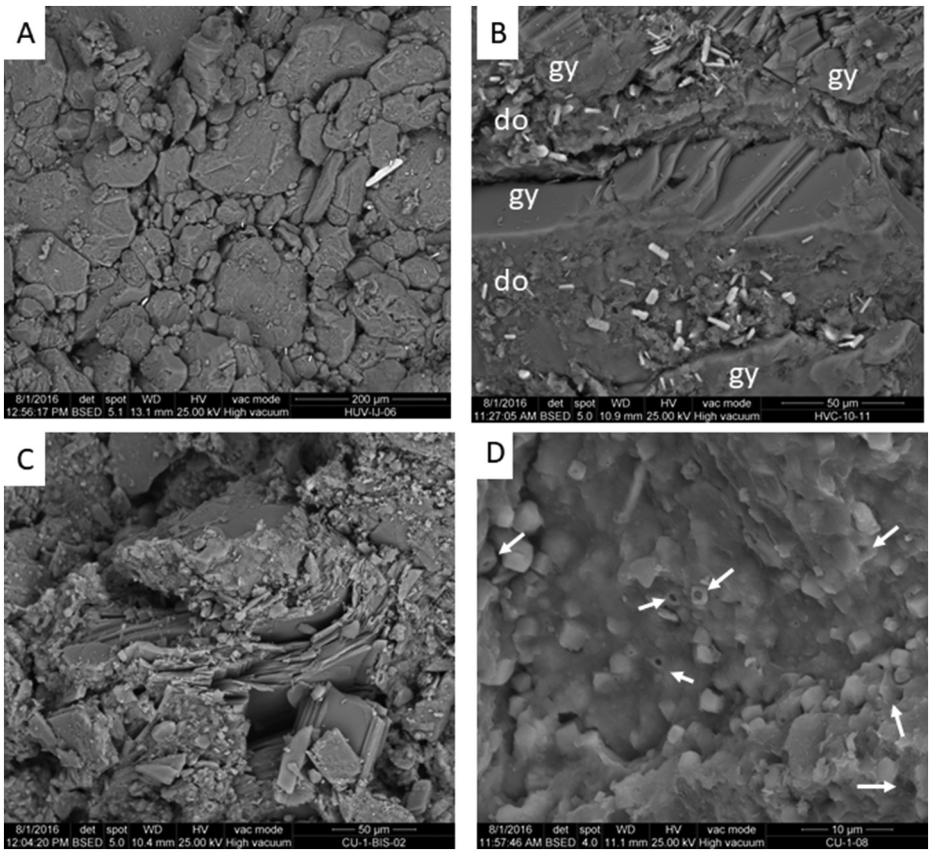

Fig. 7. Scanning electron microscope photographs of gypsarenites. A) Lenticular and subeuhedral–hemipyramidal gypsum exhibiting crystal-supported fabric. B) Gypsum crystals (gy) embedded by a matrix containing dolomite (do) and celestite crystals (white). C) Folded and cracked gypsum crystal along the (010) main cleavage. D) Smooth and continuous film embedding dolomite crystals that exhibit inner holes (arrowed).

geochemical conditions of the water (Cabestrero and Sanz-Montero, 2018). The activity of sulfate reducing bacteria and other microorganisms may also favor the corrosion and dissolution of sulfates (Sanz-Montero et al., 2006; Ayllón-Quevedo et al., 2007). To a lesser extent, the nucleation of dolomite and other carbonates, Mg-phyllosilicates and celestite also occurs on the microbial matrices of modern lakes (Sanz-Montero et al., 2013; Cabestrero and Sanz-Montero, 2018; Del Buey et al., 2021). Very often, carbonate microcrystals display hollow spheroid cores (Cabestrero and Sanz-Montero, 2018) that could represent former sites of microbial occupancy (Sanz-Montero et al., 2006; Ayllón-Quevedo et al., 2007; Sanz-Montero et al., 2009). In Miocene rocks, the good preservation of many of such features as well as fluorescent and carbonaceous films also suggest that mineral precipitation occurs in microbial biofilms. Thus, beds containing intrasediment-grown gypsum are interpreted as lithified microbial mats.

Besides, Sanz-Montero and Rodríguez-Aranda (2013) and Sanz-Montero et al. (2015) observed the formation of mat deformation structures (sensu Noffke et al., 2001) in modern gypsum-bearing microbial mats during storm events. They illustrated among others, mat fragments, wrinkle mat piles, gas domes, mud holes, scour marks, and ripple marks with complex patterns. It was also described how drapes of organic-rich mud eroded from the upper millimeters of sediment deposited between the ripple crests and depressions, resulting in the leveling of the surface (Sanz-Montero et al., 2015). In addition, the rapid overgrowth of the sedimentary structures by microbial mats (Sanz-Montero and Rodríguez-Aranda, 2013), plays a role in the biostabilization and preservation of the gypsum deposits as also reported in siliciclastic depositional environments (Noffke et al., 2001; Cuadrado et al., 2011; Cuadrado, 2020). Similar mat fragments, intraclasts, ripple marks and leveling structures are well preserved in Miocene gypsum rocks, which allow reconstructing the hydrodynamic conditions and bed forms produced by windstorms in the ancient lakes of Duero and Madrid basins.

In summary, two types of traces of life (i.e., biosignatures) are detected in Miocene gypsum deposits (Table 1): morphostructural, including MISS, and geochemical, embracing organic and inorganic signatures. The latter includes a group of bioinduced minerals that exhibit distinctive textural and compositional features. These biosignatures are also common in modern saline lakes.

4.3. Description and interpretation of synsedimentary deformation structures

In addition to MISS, gypsum beds show an association of different soft sediment deformation structures (SSDSs) and fractures that extent several kilometers laterally (Figs. 8–11). In this paper the classification of structures is based mainly on the geometry of the deformations described in siliciclastic deposits. Table 2 shows the classification along with a description of the geometry, lithologies, and the frequency of the deformation structures. Most of them appear in the two study basins, although with some particularities that are outlined in the descriptions. In general, the size and vertical repetition of deformed layers is greater in HV than in CU (Table 2).

4.3.1. Load cast structures

In the Madrid Basin, load casts develop on the lower surfaces of three gypsarenite beds (Figs. 2, 8), apparently following SE–NW directions. Load structures are often grouped in successions of 4–12 individuals separated by approximately periodic spacing that can be associated with convolute bedding features (Figs. 2, 8B, 9F).

In the Duero basin, the load casts appear as small bodies that seldom form drops and pillows collapsed into the lower beds (Fig. 10B).

Table 1
Summary of biosignatures detected in Miocene gypsum deposits.

Biosignatures	
Morphostructural (MISS)	Geochemical
Microbial laminated gypsum (Figs. 5B–D, 6A, 9D) Surface morphology related to cohesion: laminated leveling structures (Figs. 5D, F, 6A, B, D) Mat fragments (intraclasts, chips) (Figs. 6A, B, E, 11E, F) Bioweathering (corrosion) (Fig. 6B, F) Gas pits (Figs. 5F, 6H, I)	Bioinduced minerals Intrasediment-grown lenticular gypsum (Figs. 6, 7A, B) Dolomite with biomolds (Fig. 7B, D) Phyllosilicates (sepiolite, palygorskite) (Figs. 5E, 10C, E, F) Celestite (Fig. 7B) Organic films (Figs. 6B, 7B, D)

Load structures form when a higher bulk density layer rests on a layer of lower bulk density (Owen, 2003). A gravitational readjustment occurs if the shear stress of the lower layer is reduced by liquidization and thixotropic processes, commonly after a seismic shake or a rapid sedimentation event. Thus, the layer of relatively higher density collapses while the layer of lower density, that is water saturated, moves upward (Alfaro et al., 1997; Montenat et al., 2007). In the Miocene successions, the overlying gypsum is denser and more lithified than the underlying beds due to their high contents in dolomite and/or gypsum overgrowths. Rather than sudden deposition mechanisms, the biochemical precipitation of gypsum, the orientation of some pillow structures and the shallow condition of the saline lakes support an origin related to synsedimentary earthquakes.

4.3.2. Dish structures

Dish structures are generally associated to water escape conducts and small plastic intrusions of mudstone or marlstone (Figs. 9C, 10C).

The combination of the dewatering of fine-grained deposits and the compaction of sediments causes bending, breakage, and modification of the more rigid, interbedded laminae (Hurst and Cronin, 2001), in the study cases represented by gypsarenite.

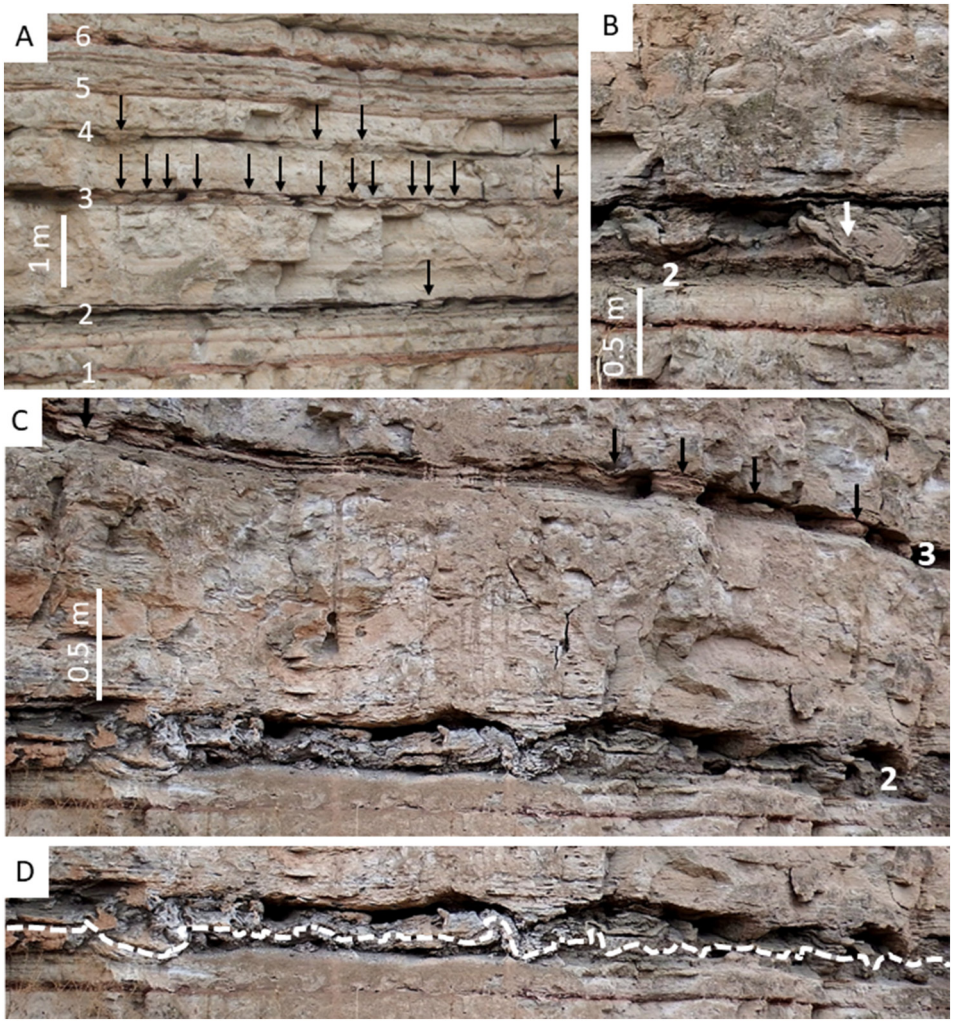

Fig. 8. Soft sediment deformation structures developed in different beds of Huerta de Valdecarábanos outcrops. The numbers correspond to the same bed in all photographs (see Fig. 2 for location). A) Load cast structures developed in gypsum interbedded with mudstone (black arrows). Periodical load casts are found in level number 3. B) Convolute bedding. An overturned syncline is observed to the right (white arrow). C) Detail of convolute bedding and load cast structures in levels 2 and 3, respectively. The outcrops shown in A and C are separated approximately 600 m. D) Drawing of a folded stratification plane shown in (C).

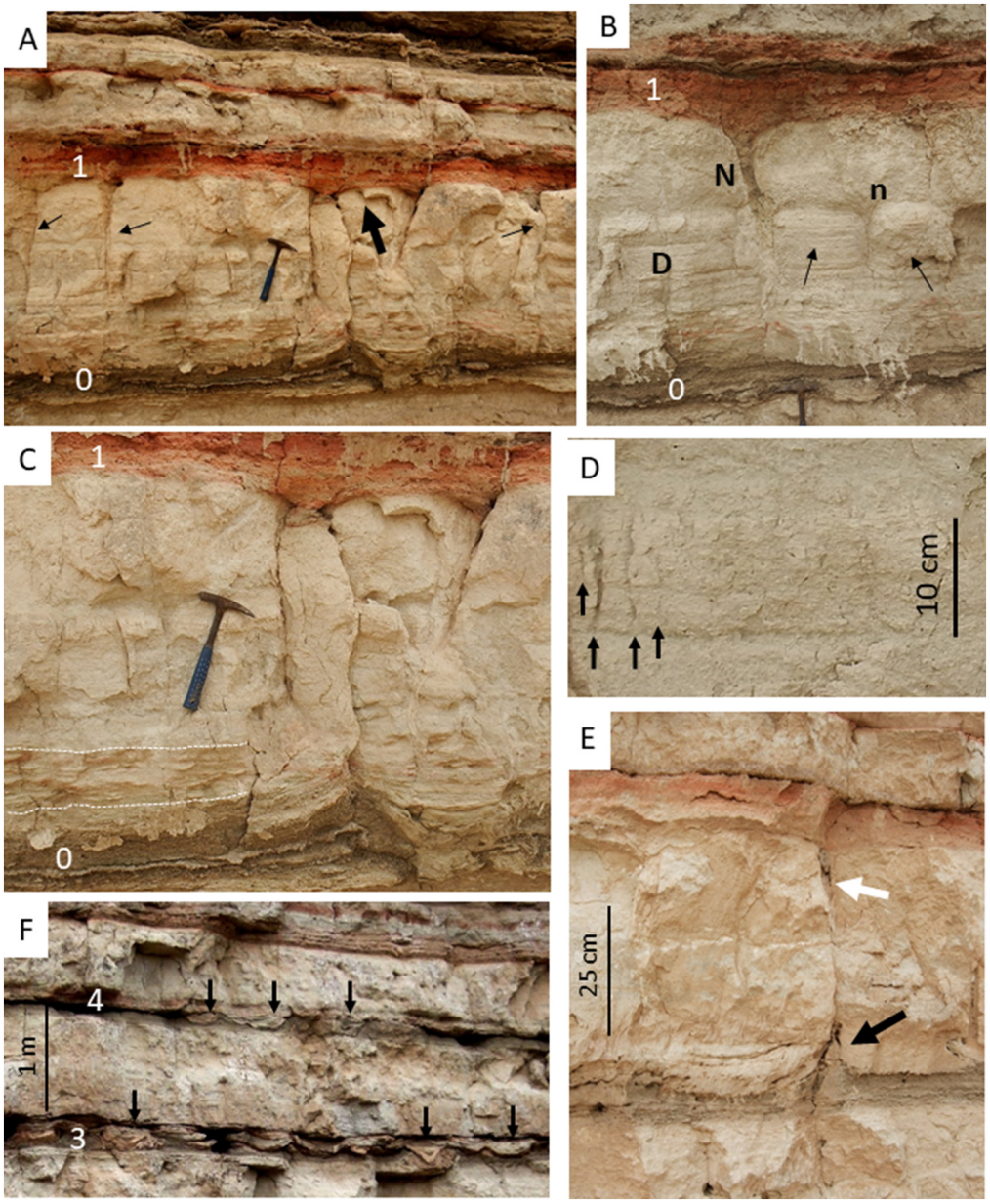

Fig. 9. Deformation structures in Huerta de Valdecarábanos outcrops. The numbers correspond to the same beds as in Fig. 2. A) Neptunian dikes (thin arrows) and small graben filled by red mudstone (coarse arrow). Hammer = 28 cm. B) "N": Neptunian dike infilled with gypsum in the lower part and mudstone from the overlying level, in the upper part. The Neptunian dike "n" is only filled by gypsiferous carbonate. Note the blocks (arrowed) delimited by Neptunian dikes and plastic intrusions. The letter D indicates the location of the photo (D). Hammer = 28 cm. C) Detail of the small graben arrowed in (A). The lamination in the uppermost part of "layer 1" is horizontal, fossilizing the graben. Notice the plastic intrusion from the mudstone "layer 0" and the dish structures at the base of the gypsum bed (between two dashed lines). D) Vertical fluid scape tubes (arrowed) parallel to synsedimentary fractures. E) Plastic intrusion (black arrow) associated to load casts occurs through a fracture. A Neptunian dike (arrowed in white) developed in the upper part of the fracture. F) Pillow structures in "layer 3" and drop like load cast in "layer 4".

4.3.3. Convolute bedding and lamination

In the Madrid basin the convoluted beds display complex folding styles such as straight, recumbent and overturned (Fig. 8B–D). Undeformed intervals of only a few meters are observed between contiguous convoluted stretches. The lower bedding surface of the deformed beds is rather flat; at the top, load casts are common (Figs. 2, 8).

In the Duero basin deformation takes the form of complex folds and pseudonodules consisting of crystalline gypsum (Figs. 3, 10C). In addition, convolution at the scale of centimeters occurs in gypsum beds with dolomite laminae that are commonly fragmented (Fig. 10A, C).

The origin of this structure is related to fluidization, dewatering and folding of a layer formed by sub-layers of different densities induced by loading, current shear, or slumping (Rossetti and Góes, 2000; Montenat et al., 2007). The occurrence of this structure in laterally continuous horizons, separated by undeformed beds, suggests a seismic trigger (Moretti and Van Loon, 2014; Shanmugam, 2016). The weak post-deformation effects of compaction observed in the folds have been further interpreted as evidence of rapid dewatering caused by earthquakes (Montenat et al., 2007). Along the same terms, lateral changes in the convoluted bed indicate different stages of fluidization, characteristic of seismic shocks (Montenat et al., 2007).

4.3.4. Fluid escape tubes

Fluid escape tubes locally run parallel to fractures (Fig. 10D). The tubes can be hollow or cemented by carbonates and gypsum (Figs. 5E, F, 9D).

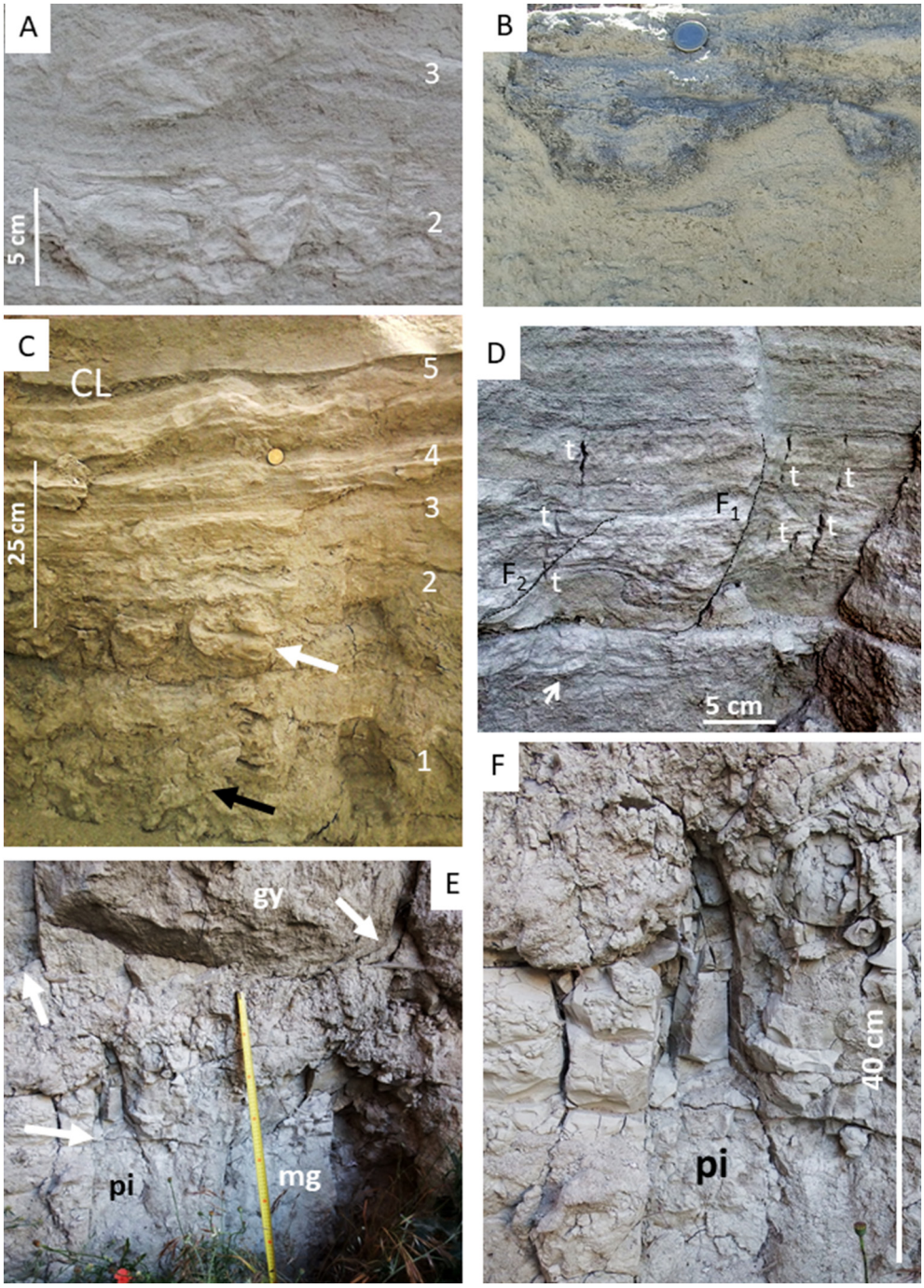

Fig. 10. Deformation structures in Cuéllar area. The numbers correspond to the same layer in all photographs (see Fig. 3 for location). A) Laminated microbialite showing convolute lamination in two layers. B) Load cast structures comprised of gypsum with high dolomite contents introduced into fine gypsarenite. Coin for scale = 23 mm. C) Photo taken a few meters from (A) showing attenuated deformation in layers 2 and 3. Dish structures and pseudonodules are arrowed in white and black, respectively. Rippled topography in gypsum beds is leveled by carbonate laminae (CL). D) Fluid scape tubes (t) are parallel to a reverse synsedimentary microfault (F1). Tubes are vertical and cut a previous fracture (F2). A dish structure is arrowed. E) Plastic intrusions (arrowed) in the lower part of the succession. "gy": gypsarenite; "mg": marlstone with gypsum. "pi": location of photo F. Scale = 70 cm. F) Detail of a plastic intrusion from previous photo (pi). Notice the chaotic structure in the upper part revealing fluidization.

These structures indicate fluid escape motion upwards, mainly because of dewatering after sediment fluidization. On occasions, fractures contribute to fluid migration. When the tubes are not associated with deformation structures, other possible mechanisms, such as rising gases within microbial mats, may have played a role in the creation of the features (Aref, 1998). The occurrence of carbonates and gypsum cements evidences seepage of fluids of different composition through the pipes. It is beyond the scope of this study to analyze the cements, although they represent an important tool to improve understanding of synsedimentary diagenesis of microbial gypsum deposits.

4.3.5. Fractures

Fractures cut specific gypsum beds that appear underlain and overlain by undeformed strata (Figs. 2–4). Locally, small reverse faults are associated to convolute bedding and lamination (Figs. 8B, C, 10D). Besides, fractures may be related to mud/sand volcanoes (Fig. 11), plastic intrusions

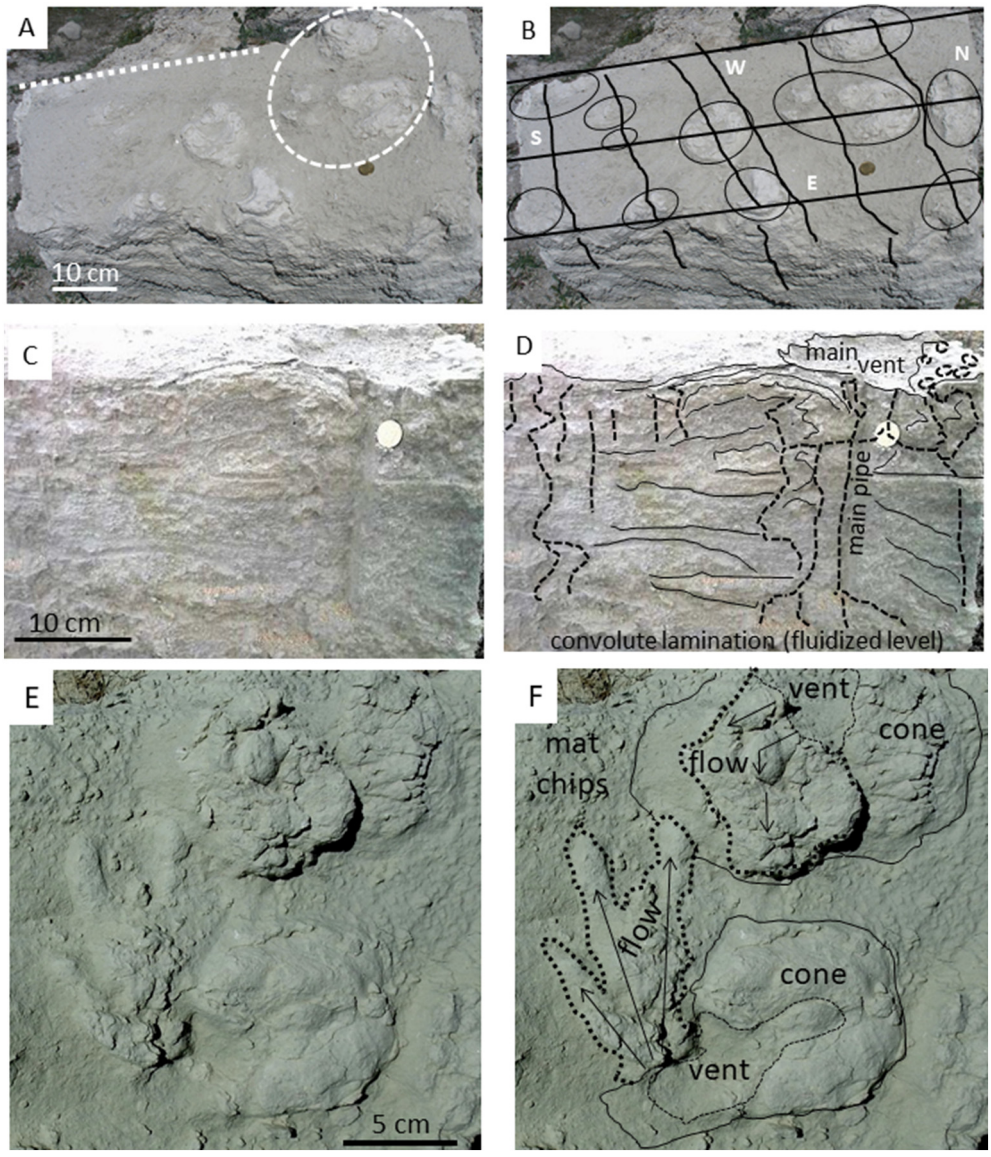

Fig. 11. Mud/sand volcanoes developed in gypsum microbialites as seen in a 3D block in Cuéllar. A) Upper bedding plane showing the vents of the volcanoes made up of white dolomite laminae. Dashed straight line marks the location of photos C and D. The volcanoes of photo (E) are encircled. B) Interpretation of (A). Notice the preferred orientation of vents along fractures and their junctions. Letters indicate cardinal points. C, D) Profile view of a mud/sand volcano showing the main pipe that connects a convoluted bed with the surface (main vent). Notice the layering of the flanks around the vent (outlined) and the association with fluid escape conducts (dashed lines). E, F) Magnified view of A showing the morphology of the volcanoes and the lobes formed by the ejected material.

(Figs. 4C, 9E) and fluid escape tubes (Fig. 10D). In HV, fractures locally define small synsedimentary grabens filled by mudstone (Fig. 9A, C).

The limited location of these joints and faults to specific beds as well as their association with other deformation structures support that they are synsedimentary features. Fractures are brittle deformation structures that indicate that the affected gypsum layers were partly lithified and rather rigid.

4.3.6. Plastic intrusions

Plastic intrusions or injectites are commonly related to one or two fractures, load casts and/or dish structures (Fig. 9C, E). In HV, they often evolve upwards to Neptunian dikes (Fig. 9A–C, E).

In CU area, the intruding material contains high percentages (ca. 50 %) of palygorskite and sepiolite (Fig. 10E, F) and occurs associated to preferentially NW–SE oriented fractures. Besides, cm-sized plastic intrusions, often occur associated with fluid escape tubes and micro-fractures (Fig. 5E).

Plastic intrusions are caused by fluidification of sediments and rising of plastic material, mainly through hydraulic fractures without clear orientation patterns (Montenat et al., 2007; Moretti and van Loon, 2014); however, in CU intrusions proceed through tectonic fractures, which supports that earthquakes are the triggering mechanism for this structure.

4.3.7. Neptunian dikes

Dikes are developed along joints or normal synsedimentary small faults (Fig. 9A–C). Locally, a plastic intrusion at the lower part of a gypsum bed is connected upwards with a Neptunian dike by the same fracture, this forming gypsum boulders and blocks (Fig. 9B, E).

Neptunian dikes form by introduction of material, either under pressure or by simple filling of pre-existing cracks or fissures from above (Montenat et al., 2007). This type of structure indicates brittle failure of cohesive or semi-lithified sediments that potentially can be triggered by different mechanisms, including desiccation cracks, seismic shocks and dehydration and hydration processes of Ca-sulfates. Multiple sediment infills, as observed in Miocene gypsum, indicate that the same sediments were affected by two or more deformation events at

Table 2
Description of deformation structures observed in the studied successions (CU: Duero Basin and HV: Madrid Basin).

Seismite	Geometry	Lithology	Frequency	Figs
Load cast and pillow structures	Sagging or drop like hemispheroids, locally pillow structures separated from the upper layer. HV: 30–50 cm wide; 10–50 cm thick. CU: up to 18 cm wide and 10 cm thick	HV: gypsarenite bodies inside gypsiferous mudstone CU: high dolomite content gypsarenite inside finer-grained gypsum	Common	8, 9, 10B
Dish structures	Concave-upward gypsarenite broken laminae; 5–15 cm in diameter; a few centimeters in thickness.	Base of gypsum microbialite layers overlying mudstone/marlstone beds or within them	Moderate	9A, C 10C, D
Convolute bedding	Up to 50 cm thick beds with complex folds, locally pseudonodules	Thin gypsum layers interbedded with mudstone or dolomitic marlstone	Common	8B–D, 10C
Convolute lamination	Ca. 5 cm thick layers with broken and folded laminae	Laminae of gypsum microbialite and dolomite	Moderate (only in CU)	10A, C, D
Fluid escape tubes	Vertical or oblique cylindrical contorted tubes. Length in section < 100 mm. Diameter = 3–15 mm	Gypsum microbialite and dolomitic marlstone	Common	5E, F, 6I, 9D, 10D, 11C, D
Synsedimentary fractures	Subvertical and curved joints or cm-slip normal faults. Locally, reverse microfaults	Mainly gypsum microbialite beds. Locally, mudstone and marlstone	Common	4, 9A, C, E, 10D–F, 11
Plastic intrusions	Flame/triangular morphology, up to 40 cm wide, up to 60 cm high	Clay-silt or marl intruding into an overlying gypsum microbialite or marlstone layer	Common	4C, 5E, 9C, E, 10E, F
Neptunian dikes	15–80 cm long and up to 15 cm wide cracks cutting perpendicularly the gypsum host and open upwards like a wedge	Simple gypsiferous infill or a mixed infill, where the uppermost cm have the same clay/silt composition that the layer that seals the crack	Scarce (only in HV)	6G, 9A–C, E
Mud/sand volcanoes	Rounded piles 5–10 cm in diameter and up to 5 cm high; Volcanoes display an irregular central vent and small lobes of mud that flow from it	Host rock: gypsum microbialite. Extruded sediment: lenticular gypsum with high dolomite content.	Scarce (only in CU)	6H, I, 11
Microstylolites	Complex, serrated, irregular, pressure-dissolution surfaces, approximately parallel to bedding, 250 μm wide discontinuous bands	Films of dolomicrite, clay and iron oxides in gypsum microbialites	Scarce (only in HV)	6D

different stages of early diagenesis (Montenat et al., 2007; Törő and Pratt, 2016). The association of this structure with synsedimentary faults and plastic intrusions suggests that they were produced by seismic shakes; although their formation could be facilitated from previous structures such as mudcracks or, just the opposite, desiccation cracks developed preferentially along fractures induced by earthquakes.

4.3.8. Microstructures: stylolites and deformed gypsum crystals

Microscope studies evidence the presence of microstylolites in HV rock and deformation of gypsum crystals in CU. Three main types of deformation of crystals have been detected: folding, displacement of planes and cracking of crystals, along the (010) main cleavage (Figs. 6E, 7C).

It is accepted that stylolites parallel or horizontal with respect to bedding plane are produced by the pressure generated by overlying rocks during burial (Toussaint et al., 2018). Although there have been many studies on Miocene lacustrine deposits of the Madrid Basin, this is the first-time that stylolites have been reported. This would be because the thickness of overburden rocks in the study successions (<80 m) is not enough to produce such structures. Along these lines, Montenat et al. (2007) and Seilacher (1969, 1984) suggested that earthquakes can produce a sudden increase in compaction without an effect of overloading. Accordingly, accommodation to compaction strain during seismic shocks seems the most plausible mechanism for the formation of the microstylolites and the deformation of gypsum crystals in the study successions. In this way, it is interpreted that gypsum crystals deformed differently depending on the orientation of the crystals and their (010) cleavage. If the vertical stress was parallel to cleavage, the fragments moved along such planes without separating (Fig. 6E). Alternatively, when stress was oblique, crystals broke, and their fragments separated (Fig. 6E). The type of deformation as well as the different orientations and specific location of the fragmented crystals in Miocene beds allow discarding reworking and mineral replacements. Such mechanisms were adduced by Aref and Mannaa (2021) as the responsible for the fragmentation of crystals in sabkhas.

4.3.9. Mud/sand volcanoes

A group of mud/sand volcanoes is uniquely exposed in three dimensions in Cuéllar succession, which allowed visualizing the surficial and internal structures of these edifices (Figs. 3, 11) as well as their alignment, along fracture directions (Fig. 11B). They occur associated to mat flakes and gas tubes (Fig. 11E, F). In cross-section, layers around the vent tilt steeply downwards (Fig. 11C, D). Vertical and subvertical pipes up to 6 cm long, connect the central plug of the volcanoes with an underlying bed showing convolute lamination that appeared as the source of the ejected sediment (Fig. 11C, D). The main conducts occur at fracture intersections surrounded by several secondary tubes (Fig. 11B, D). Observations of the pipes infilling under a light microscope reveal that ejected gypsum crystals and dolomite matrix are crossed by oriented micro-cracks and micro-tubes (Fig. 6H, I).

Mud volcanoes typically occur where stratified rocks with an abundance of water-saturated sediment, commonly consisting of uncemented mud and sand, are under pressure from overlying strata. The cones form as the fluidized sediment is extruded through a vent at the sediment surface (Montenat et al., 2007; Moretti and van Loon, 2014; Taj et al., 2014). In the Miocene rocks it has been shown that the overpressured sediment was comprised of an uncommon mixture of dolomite and gypsum. As in many other sedimentary volcanoes, the fluidized mixture intruded the overlying bed through fractures acting as preferentially conduits (Montenat et al., 2007; Moretti and van Loon, 2014). Tides, storms and seismic shocks cause the release of pressure from a liquified unit (Shanmugam, 2017). The carbonatic lithology of the edifices and the occurrence of mat flakes provide evidence of microbial mats on the upper surface of the bed. The impermeable and cohesive surface of the mats is reported to trap gases that increase the pore pressure and can destabilize the underlying sediment (Montague et al., 1993). The fragmentation of the microbial layer and sudden exposure of bubble-separated sediment trigger water-saturated injection of sediment (Taj et al., 2014). A similar effect of gas blistering and destabilization of sediment due to the fragmentation of microbial mats following storm events has been reported in modern lakes where gypsum microbialites are forming (Sanz-Montero and Rodríguez-Aranda, 2013; Sanz-Montero et al., 2015). Albeit in many ancient microbialites it may be difficult to discriminate between microbial and seismic structures (Moretti and van Loon, 2014), in Cuéllar a range of features provide criteria to interpret this structure as seismites, among others, the association of volcanoes with other deformation structures and the preservation of the central pipe linking the surface with a deeper source. At microscale, the net of fractures and pores also provides evidence of a seismic shock. Besides, the preferred orientation of gypsum crystals along the pipes reveals main flow directions (Fig. 6H, E).

5. Discussion

Miocene lacustrine gypsum rocks of Madrid and Duero basins contain a remarkable record of biosignatures and microbially induced sedimentary structures. These structures indicate variable sedimentary conditions that are interpreted to range from calm submerged environments, where intrasedimentary gypsum grows, to stormy situations reflected by cross stratification. Besides, this study provides the first evidence of deformation structures indicative of earthquakes in microbial gypsum deposits. The distribution of seismites in two separated sequences gives accurate insight into the seismogenic behavior of the gypsum microbial sediments and faults in areas devoid of silt to sand sized siliciclastic deposits.

5.1. Microbialite development in shallow hypersaline lakes and preservation

Reports of modern and shallow hypersaline settings show that gypsum grows within microbial mats forming laminated deposits (Ortí et al., 1984; Gerdes et al., 2000; Rouchy and Monty, 2000; Sanz-Montero et al., 2013; Cabestrero et al., 2018; Del Buey et al., 2021). The morphology of these deposits is commonly altered and the microbial fossils rarely preserved in the geological record that may make their interpretation difficult (Gerdes et al., 2000; Rouchy and Monty, 2000). Albeit, this study based on a comparison of Miocene gypsum successions and modern analogs, particularly those found in the shallow hypersaline lakes of center Spain, reveals that a suite of mineralogical and chemical biosignatures as well as microbial induced sedimentary structures can be preserved in gypsum rocks. Combining such attributes allowed the reliable identification of Miocene gypsum beds as microbialites. Among the mineralogical biosignatures, it is remarkable the preservation of intrasediment-grown lenticular gypsum crystals associated to organic matrix and inclusions (Ortí et al., 1984; Rouchy and Monty, 2000; Del Buey et al., 2021). Besides, the mineralogical assemblages of Miocene rocks comprised of gypsum, dolomite, celestite, Mg-clays and ankerite are quite similar in modern sedimentary environments, where the precipitation of each of these minerals has been reported to be related with bacterial activities (Rouchy and Monty, 2000; Sanz-Montero et al., 2008, 2013; Petrash et al., 2012; Cabestrero and Sanz-Montero, 2018; Del Buey et al., 2018, 2021). Regardless of the mechanisms for their formations, the progressive precipitation of minerals causes the early lithification of the microbial mats and, thus, favors their preservation in the fossil record. Notably, laminae mineralized in carbonates, which appear with continuous and undulated surface morphologies, show higher lithification and rigidity degrees than gypsum beds. These different physical properties may explain the distinct behavior of each type of sediment upon deformation. Direct observation of the interplay between gypsiferous sediments and wind-driven currents in shallow lakes, showed that currents were sufficient to erode away the microbial mats producing mat fragments, abraded crystals, scours and ripple forms, among other structures (Sanz-Montero and Rodríguez-Aranda, 2013; Sanz-Montero et al., 2015). The abundance of *cross* bedding structures in gypsum strata highlights the crucial role of the hydrodynamic conditions induced by episodic storms had on the sediment accumulation in the Miocene lakes of central Spain. As in siliciclastic deposits (Noffke, 2010), it has been observed that organic mud drapes infill the ripple troughs in the saline lakes (Sanz-Montero et al., 2015). The accumulation of drapes together with the rapid recolonizing of the bedforms conducts surface leveling (Noffke et al., 2001) as well as the biostabilization and the persistence of structures in the sedimentary environments (Cuadrado et al., 2011). The good preservation of the sedimentary forms in Miocene gypsum deposits of the two study successions suggests that biostabilization may enhance the potential of preservation of gypsum beds that would otherwise have been easily eroded away.

5.2. SSDSs and brittle structures interpreted as seismites

A wide range of sedimentary deformation structures are found in the Miocene gypsiferous deposits: load casts, pillows, dish structures, convolute bedding and lamination, plastic intrusions, fluid escape tubes, mud/sand volcanoes, horizontal microstylolites, Neptunian dikes and fractures. These structures reflect ductile and brittle (microfractures) deformation or a combination of both types. The latter applies for plastic intrusions associated to the formation of Neptunian dikes and fractures, which occur either simultaneously or during successive deformational stages (van Loon, 2009).

According to Shanmugam (2016), liquefaction can be induced by many triggering mechanisms besides earthquakes. In the study cases most of such mechanisms can be ruled out easily based on the abundance of horizontally bedded primary gypsums, the wide lateral extent of deformations (Moretti and van Loon, 2014; Shanmugam, 2016), the shallow condition of the lacustrine settings, the lack of evidence of depositional slopes, the shallow burial diagenesis and the geographical and temporal separation between the two sedimentary successions. Care has been taken to interpret ductile deformation features as seismites, where there are other potential candidates for forming them. Thereby, the preferential location of the Miocene sand volcanoes at the intersection of fractures in the CU area suggests a seismic trigger to the detriment of accumulation of gases in the microbial mats, as reported by Taj et al. (2014). Similarly, load cast and pillow structures tend to follow specific directions in HV. Besides, convolute bedding and lamination structures could be caused by storm episodes (Alfaro et al., 2002), but in Miocene rocks these features occur associated with brittle deformation structures, which gives criteria for interpreting them as seismites.

The distribution of the outcrops along NW–SE trending fault systems (Fig. 1B) that were tectonically active during the sedimentation of the gypsum deposits provides a key and additional indicator of potential seismic shocks. Active strike-slip faults in the region reflect Variscan fractures reactivated during the Alpine orogeny (De Vicente et al., 2011). Along the same lines, the occurrence of an overlying interval of gently dipping beds that laterally disappear in CU points to synsedimentary tectonic activity (e.g., Montenat et al., 2007) and reveals a substantial change in the type of sediment infill. In HV the abrupt accumulation of mudstone over gypsum deposits also indicates tectonic-driven changes in the depositional setting. So, these results point out the dominant role of tectonic-driven changes in saline lakes devoid of fossils other than microbes.

Besides, gypsum beds show distinctive microstructural features such as horizontal microstylolites and cracked gypsum crystals that provide a new type of evidence for synsedimentary tectonic activity in gypsum deposits. The vertical orientation of gypsum lenses in the sand volcanoes and Neptunian dike infills is another microstructural tool for identifying injection of material under pressure in ancient rocks. Infilling by vertically oriented lenses in dikes is different from bioturbation traces typically found in ancient and modern gypsiferous lakes (Rodríguez-Aranda and Calvo, 1998; Sanz-Montero et al., 2013). In gypsum lakes, extensive bioturbation is mainly caused by invertebrates and produces distinctive meniscate back-filled tubes arranged in all directions that aid in their recognition (Rodríguez-Aranda and Calvo, 1998; Sanz-Montero et al., 2013).

Thus, a combination of lithologic, sedimentary, stratigraphic and micro to macro structural criteria allows interpreting SSDSs and brittle structures as seismites. Many reports document the occurrence of seismites in siliciclastic sediments associated with microbialites deposited in different sedimentary conditions (Eriksson and Truswell, 1974; Alvaro et al., 2006; van Loon et al., 2016). As far as we know, this study provides the first example of deformation structures affecting a mix of lithologies dominated by primary gypsum sediments deposited in shallow saline lakes and gives insight into the high susceptibility of intrasediment-grown gypsum deposits to liquefaction. According to

the study of mechanical behavior of silt sized gypsum sediments in modern saline lakes conducted by Pulmariño et al. (2019), gypsum sediments display higher cohesion properties than fine sized siliciclastic sediments. The research also demonstrated that cohesion of gypsum deposits changes very little with the moisture contents. The lenticular morphology of gypsum crystals offering higher resistance to particle separation could be behind this behavior (Pulmariño et al., 2019). Such results suggest that gypsum sediments may be less susceptible to liquefaction than weakly consolidated siliciclastic grains. Therefore, they would need larger magnitude earthquakes to form. Martín-Banda et al. (2008) reported siliciclastic deposits showing syndepositional deformation structures (load casts, pillows and convolute bedding) associated to the E–W trending faults in the southern border of the Madrid Basin (Fig. 1). Distant 30 km from HV, such structures are slightly older (Miocene Lower Unit) and of relatively larger scale (meter scale) than the ones formed in the studied gypsum facies.

It is assumed that seismic shocks that affect several tens of kilometers from the epicenter, as in the study areas, had a moderate-to high-magnitude (Moretti and van Loon, 2014; Shanmugam, 2016). Along the same terms, Rodríguez-Pascua et al. (2000) and Montenat et al. (2007) suggested that the threshold for seismically-induced liquefaction corresponds to a magnitude over 5, though depending on the attributes of the affected sediments. Synsedimentary brittle structures indicate that the lithification degree of sediments was varied in the study areas upon deformation. Plastic intrusions (Figs. 4C, 8C, E) and lenticular gypsum crystals arranged parallel to the fracture surface (Fig. 6G) reveal unconsolidated ground, but Neptunian dikes and microfaults (Fig. 8A, B) are typical of more compacted sediments (Montenat et al., 2007). The degree of lithification of the rocks is useful to assign the intensity of an earthquake using the Modified Mercalli Scale. It is estimated that fractures in lithified rocks, like in cemented gypsum and dolomite laminae, are produced by earthquakes with intensities above VIII (Michetti et al., 2007; Silva and Rodríguez-Pascua, 2014).

In sedimentary environments it is difficult to specify the number of seismic shocks because their effects can reach several meters deep and a single earthquake can produce superposed deformed beds (Montenat et al., 2007; Alfaro et al., 2010; Gibert et al., 2011), though the pattern of distribution of deformed layers through the Miocene successions points to close shocks (Bose et al., 1997; Owen, 1996; Seilacher, 1984). As inferred from differences in the number and typology of seismites between the two areas, earthquakes were stronger and less frequent in HV than in CU (Figs. 2, 3). The larger magnitude and lower recurrence periods of earthquakes recorded in HV with respect to CU could be related with discontinuous fault movements and longer periods of strain accumulation in the fracture plane.

These results reveal the dominant role of tectonic-driven changes may have in saline lake sedimentation. In addition, results help to understanding the seismogenic behavior of both gypsarenites and faults in areas devoid of siliciclastic deposits during successive deformational stages.

6. Conclusions

The study of two Miocene sedimentary successions in the Duero and Madrid Basins reveals that a suite of microbial induced sedimentary structures (MISS) can be finely preserved in lacustrine deposits comprising sandy gypsum crystals. The MISS identified in the two separated successions, such as ripple leveling, mat clasts, and others, provide ancient analogs for modern gypsum microbialites formed in saline and shallow lakes, subjected to periodic storm influence. The rapid mineralization of the microbial mats and biostabilization processes may play a role in the good preservation of the depositional structures in sulfates that would otherwise have been altered or vanished.

Besides, the successions show large-scale deformation structures (SSDSs and fractures), reflecting ductile and brittle deformation. The combination and spatial distribution of these structures nearby active strike-slip faults allow interpreting deformation features as true seismites. Those identified in the Duero Basin include small fractures, load casts, pillows, dish structures, convolute bedding and lamination, plastic intrusions, fluid escape tubes and mud/sand volcanoes. The latter is absent in the Madrid Basin, by contrast, this succession shows Neptunian dikes and horizontal microstylolites. The difference of types and higher vertical repetition of deformation structures in the Duero Basin than in the Madrid Basin suggest that earthquakes were stronger and less frequent in the latter.

The abundance of SSDSs in the two successions gives evidence that gypsum microbial sediments are highly prone to earthquakes. Thus, the vertical distribution of the deformation structures provides a good record of the seismogenic behavior of faults. The association of MISS and SSDSs gives unique information for understanding the evolution and paleoenvironmental conditions of saline lakes and their basins.

Declaration of competing interest

The authors declare that they have no competing financial interests or personal relationships that could have influenced the present research work.

Acknowledgements

This research is dedicated to MESM's deceased mother, who was a great companion during fieldwork in Cuéllar. We much appreciate comments and fieldwork assistance provided by Dr. Afify in the Madrid Basin. Comments by Dr Aref and an anonymous reviewer greatly contributed to improve the manuscript. Finnancial support from the Complutense University of Madrid to the Research Group UCM-910404 is acknowledged.

References

Alfaro, P., Soria, J.M., Moretti, M., 1997. Soft-sediment deformation structures induced by earthquakes (seismites) in Pliocene lacustrine deposits (Guadix-Baza Basin, Central Betic Cordillera). Eclogae Geologicae Helvetiae 90, 531–540.

Alfaro, P., Delgado, J., Estévez, A., Molina, J.M., Moretti, M., Soria, J.M., 2002. Liquefaction and fluidization structures in Messinian storm deposits (Bajo Segura Basin, Betic Cordillera, southern Spain). International Journal of Earth Sciences 91, 505–513.

Alfaro, P., Gibert, L., Moretti, M., García-Tortossa, F.J., Sanz de Galdeano, C., Galindo-Zaldívar, J., López-Garrido, A.C., 2010. The significance of giant seismites in the Plio–Pleistocene Baza palaeo-lake (S Spain). Terra Nova 22 (3), 172–179.

Allen, J.R.L., 1982. Sedimentary Structures: Their Character and Physical Basis. Vol. II. Elsevier, p. 663.

Allwood, A.C., Burch, I.W., Rouchy, J.M., Coleman, M., 2013. Morphological biosignatures in gypsum: diverse formation processes of messinian (6.0 Ma) gypsum stromatolites. Astrobiology 13, 870–886.

Alvaro, J.J., Clausen, S., El Albani, A., El Hassane, C., 2006. Facies distribution of the Lower Cambrian cryptic microbialand epibenthic archaeocyathan-microbial communities, western Anti-Atlas, Morocco. Sedimentology 53, 35–53.

Aref, M.A.M., 1998. Holocene stromatolites and microbial laminites associated with lenticular gypsum in a marine-dominated environment, Ras El Shetan area, Gulf of Aqaba, Egypt. Sedimentology 45, 245–262.

Aref, M.A., Mannaa, A.A., 2021. The significance of gypsum morphology in interpreting environmental changes caused by human construction, Red Sea coastal evaporation environment, Saudi Arabia. Environment and Earth Science 80, 47.

Aref, M.A., Taj, R.J., Mannaa, A.A., 2020. Sedimentological implications of microbial mats, gypsum, and halite in Dhahban solar saltwork, Red Sea coast, Saudi Arabia. Facies 66, 10.

Armenteros, I., 1991. Contribucion al conocimiento del Mioceno lacustre de la Cuenca terciaria del Duero (sector centro-oriental, Valladolid-Penafiel-Sacramenia-Cuellar). Acta Geológica Hispánica 26 (2), 97–131.

Armenteros, I., Corrochano, A., Alonso-Gavilán, G., Carballeira, J., Rodríguez, J.M., 2002. Duero basin (northern Spain). In: Gibbons, W., Moreno, T. (Eds.), The Geology of Spain. Geological Society of London, pp. 309–315.

Ayllón-Quevedo, F., Souza-Egipsy, V., Sanz-Montero, M.E., Rodríguez-Aranda, J.P., 2007. Fluid inclusion analysis of twinned selenite gypsum beds from the Miocene of the Madrid basin (Spain). Implication on dolomite bioformation. Sedimentary Geology 201, 212–230.

Babel, M., 2004. Models for evaporite, selenite and gypsum microbialite. Acta Geologica Polonica 54 (2), 219–249.

Bachmann, G.H., Aref, M.A.M., 2005. A seismite in Triassic gypsum deposits (Grabfeld Formation, Ladinian), southwestern Germany. Sedimentary Geology 180, 75–89.

Bose, P.K., Banerjee, S., Sarkar, S., 1997. Slope-controlled seismic deformation and tectonic framework of deposition: Koldaha Shale, India. Tectonophysics 269, 151–169.
Cabestrero, Ó., Sanz-Montero, M.E., 2018. Brine evolution in two inland evaporative environments: influence of microbial mats in mineral precipitation. Journal of Paleolimnology 59, 139–157.
Cabestrero, Ó., del Buey, P., Sanz-Montero, M.E., 2018. Biosedimentary and geochemical constraints on the precipitation of mineral crusts in shallow sulphate lakes. Sedimentary Geology 366, 32–46.
Calvo, J.P., Alonso-Zarza, A.M., García del Cura, M.A., Ordóñez, S., Rodríguez-Aranda, J.P., Sanz-Montero, M.E., 1996. Sedimentary evolution of lake systems through the Miocene of the Madrid Basin: paleoclimatic and paleohydrological constraints. In: Friend, P.F., Dabrio, C.J. (Eds.), Tertiary Basins of Spain: The Stratigraphic Record of Crustal Kinematics. Cambridge University Press, Cambridge, pp. 272–277.
Cuadrado, D.G., 2020. Geobiological model to ripple genesis and preservation in a heterolithic sedimentary sequence in a supratidal área. Sedimentology 67, 2747–2763.
Cuadrado, D.G., Carmona, N.B., Bournod, C., 2011. Biostabilization of sediments by microbial mats in a temperate siliciclastic tidal flat, Bahia Blanca estuary (Argentina). Sedimentary Geology 237, 95–101.
De Vicente, G., Muñoz-Martín, A., 2013. The Madrid Basin and the Central System: a tectonostratigraphic analysis from 2D seismic lines. Tectonophysics 602, 259–285.
De Vicente, G., Cloetingh, S., Van Wees, J.D., Cunha, P.P., 2011. Tectonic classification of Cenozoic Iberian foreland basins. Tectonophysics 502, 38–61.
Del Buey, P., Cabestrero, Ó., Arroyo, X., Sanz-Montero, M.E., 2018. Microbially induced Palygorskite–Sepiolite authigenesis in modern hypersaline lakes (Central Spain). Applied Clay Science 160, 9–21.
Del Buey, P., Sanz-Montero, M.E., Braissan, O., Cabestrero, Ó., Visscher, P.T., 2021. The role of microbial extracellular polymeric substances on formation of sulfate minerals and fibrous Mg-clays. Chemical Geology 581, 120.
El Taki, H., Pratt, B.R., 2012. Syndepositional tectonic activity in an epicontinental basin revealed by deformation of subaqueous carbonate laminites and evaporites: seismites in Red River strata (Upper Ordovician) of southern Saskatchewan, Canada. Bulletin of Canadian Petroleum Geology 60, 37–58.
Eriksson, K.A., Truswell, J.F., 1974. Tidal flat associations from a Lower Proterozoic carbonate sequence in South Africa. Sedimentology 21, 293–309.
Gerdes, G., Krumbein, W.E., Noffke, N., 2000. Evaporite microbial sediments. In: Riding, R.E., Awramik, S.M. (Eds.), Microbial Sediments. Springer, Berlin, pp. 196–208.
Gibert, L., Alfaro, P., García-Tortosa, F., Scott, G., 2011. Superposed deformed beds produced by single earthquakes (Tecopa basin, California, USA). Sedimentary Geology 235, 148–159.
Grey, K., Awramik, S.M., 2020. Handbook for the Study and Description of Microbialites. Geological Survey of Western Australia, p. 147 (290 pp.).
Hurst, A., Cronin, B.T., 2001. The origin of consolidation laminae and dish structures in some deep-water sandstones. Journal of Sedimentary Research 71, 136–143.
Martín-Banda, R., Rodríguez-Pascua, M.A., López Olmedo, F., Montes, M., 2008. Sismitas antiguas (Aragoniense) en la Cuenca del Tajo, un ejemplo de sismicidad intraplaca moderada-alta. Toledo (España). Geo-Temas 10, 1067–1070.
Mediavilla, R.M., 1986-1987. Sedimentología de los yesos del sector central de la Depresión del Duero. Acta Geológica Hispánica 21-22, 35–44.
Michetti, A.M., Esposito, E., Guerrieri, L., Porfido, S., Serva, L., Tatevossian, R., Vittori, E., Audemard, F., Azuma, T., Clague, J., Comerci, V., Gurpinar, A., McCalpin, J., Mohammadioun, B., Morner, N.A., Ota, Y., Roghozin, E., 2007. Intensity Scale ESI 2007. In: Guerrieri, L., Vittori, E. (Eds.), Memorie Descrittive Carta Geologica d'Italia. APAT, Servizio Geologico d'Italia— Dipartimento Difesa del Suolo, Roma, Italy, p. 74 (53 pp.).
Montague, C.L., Paulic, M., Parchure, T.M., 1993. The stability of sediments containing microbial communities: initial experiments with varying light intensity. Coastal and Estuarine Studies 42, 348–359.
Montenat, C., Barrier, P., d'Estevou, P.O., Hibsch, C., 2007. Seismites: an attempt at critical analysis and classification. Sedimentary Geology 196, 5–30.
Moretti, M., Alfaro, P., Owen, G., 2016. The environmental significance of soft-sediment deformation structures: key signatures for sedimentary and tectonic processes. Sedimentary Geology 344, 1–4.
Moretti, M., van Loon, A.J., 2014. Restrictions to the application of 'diagnostic' criteria for recognizing ancient seismites. Journal of Palaeogeography 3, 162–173.
Muñoz, J.L., Lendínez, A., Cabra, P., 2007. Mapa Geológico de España E. 1:50.000, Cuéllar (H-401). Instituto Geológico y Minero de España (70 pp.).
Noffke, N., 2010. Microbial Mats in Sandy Deposits From the Archean Era to Today. Springer, New York.
Noffke, N., Gerdes, G., Klenke, T., Krumbein, W.E., 2001. Microbially induced sedimentary structures—a new category within the classification of primary sedimentary structures. Journal of Sedimentary Research 71, 649–656.
Ortí, F., Pueyo, J.J., Geisler-Cussey, D., Dulau, N., 1984. Evaporitic sedimentation in the coastal salinas of Santa Pola (Alicante, Spain). Revista D'Investigacions Geologiques 38-39, 169–220.
Owen, G., 1996. Experimental soft-sediment deformation: Structures formed by the liquefaction of unconsolidated sands and some ancient examples. Sedimentology 43, 279–293.
Owen, G., 2003. Load structures: gravity-driven sediment mobilization in the shallow subsurface. In: Van Rensbergen, P., Hillis, R.R., Maltman, A.J., Morley, C.K. (Eds.), Subsurface Sediment Mobilization. Geological Society of London Special Publicationvol. 216, pp. 21–34.
Peryt, T.M., Jasionowski, M., 1994. In situ formed and redeposited gypsum breccias in the Middle Miocene Badenian of southern Poland. Sedimentary Geology 94, 153–163.
Peryt, T.M., Kasprzyk, A., 1992. Earthquake-induced resedimentation in the Badenian (Middle Miocene) gypsum of southern Poland. Sedimentology 39, 235–249.
Petrash, D.A., Gingras, M.K., Lalonde, S.V., Orange, F., Pecoits, E., Konhauser, K.O., 2012. Dynamic controls on accretion and lithification of modern gypsum-dominated thrombolites, Los Roques, Venezuela. Sedimentary Geology 245, 29–47.
Pulmariño, Á., Tsige, M., Sanz-Montero, M.E., 2019. Propiedades geotécnicas de los sedimentos de la laguna Altillo Chica (Toledo): implicación en la formación de estructuras de erosión. Geogaceta 66, 139–142.
Rodríguez-Aranda, J.P., Calvo, J.P., 1998. Trace fossils and rhizoliths as a tool for sedimentological and palaeoenvironmental analysis of ancient continental evaporite successions. Palaeogeography Palaeoclimatology Palaeoecology 140, 383–399.
Rodríguez-Aranda, J.P., Calvo, J.P., Sanz-Montero, M.E., 2002. Lower Miocene gypsum paleokarst in the Madrid Basin (central Spain): dissolution diagenesis, morphological relics and karst end products. Sedimentology 49, 1385–1400.
Rodríguez-Pascua, M.A., Calvo, J.P., De Vicente, G., Gómez-Gras, D., 2000. Soft-sediment deformation structures interpreted as seismites in lacustrine sediments of the Prebetic Zone, SE Spain, and their potential use as indicators of earthquake magnitudes during the Late Miocene. Sedimentary Geology 135, 117–135.
Rossetti, D.F., Góes, A.M., 2000. Deciphering the sedimentological imprint of paleoseismic events: an example from the Aptian Codo' Formation, northern Brazil. Sedimentary Geology 135, 137–156.
Rouchy, J.M., Monty, C., 2000. Gypsum microbial sediments: Neogene and modern examples. In: Riding, R.E., Awramik, S.M. (Eds.), Microbial Sediments. Springer-Verlag, pp. 209–216.
Rouchy, J.M., Pierre, C., Sommer, F., 1995. Deep-water resedimentation of anhydrite and gypsum deposits in the Middle Miocene (Belayim Formation) of the Red Sea, Egypt. Sedimentology 42, 267–282.
Sanz-Montero, M.E., 1996. Sedimentología de las formaciones neógenas del Sur de la Cuenca de Madrid. CEDEX. Monografías 52 (245 pp.).
Sanz-Montero, M.E., Rodríguez-Aranda, J.P., 2013. The role of microbial mats in the movement of stones on playa lake surfaces. Sedimentary Geology 298, 53–64.
Sanz-Montero, M.E., Rodríguez-Aranda, J.P., Calvo, J.P., Ordóñez, S., 1994. Tertiary detrital gypsum in the Madrid Basin, Spain; criteria for interpreting detrital gypsum in continental evaporitic sequences. In: Renaut, R.W., Last, W.M. (Eds.), Sedimentology and Geochemistry of Modern and Ancient Saline Lakes. SEPM Special Publicationvol. 50, pp. 217–228.
Sanz-Montero, M.E., Rodríguez-Aranda, J.P., Calvo, J.P., 2006. Mediation of endoevaporitic microbial communities in early replacement of gypsum by dolomite: a case study from Miocene lake deposits of the Madrid Basin, Spain. Journal of Sedimentary Research 76, 1257–1266.
Sanz-Montero, M.E., Rodríguez-Aranda, J.P., García del Cura, M.A., 2008. Dolomite-silica stromatolites in Miocene lacustrine deposits from the Duero Basin, Spain: the role of organotemplates in the precipitation of dolomite. Sedimentology 55, 729–750.
Sanz-Montero, M.E., Rodríguez-Aranda, J.P., García del Cura, M.A., 2009. Bioinduced precipitation of barite and celestite in dolomite microbialites: examples from Miocene lacustrine sequences in the Madrid and Duero Basins, Spain. Sedimentary Geology 222, 138–148.
Sanz-Montero, M.E., Calvo, J.P., García del Cura, M.A., Ornosa, C., Outeruelo, R., Rodríguez-Aranda, J.P., 2013. The rise of the diptera-microbial mat interactions during the Cenozoic: consequences for the sedimentary record of saline lakes. Terra Nova 25, 465–471.
Sanz-Montero, M.E., Cabestrero, Ó., Rodríguez-Aranda, J.P., 2015. Sedimentary effects of flood-producing windstorms in playa lakes and their role in the movement of large rocks. Earth Surface Processes and Landforms 40, 864–875.
Seilacher, A., 1969. Fault-graded beds interpreted as seismites. Sedimentology 13, 15–159.
Seilacher, A., 1984. Sedimentary structures tentatively attributed to seismic events. Marine Geology 55, 1–12.
Shanmugam, G., 2016. The seismite problem. Journal of Palaeogeography 5, 318–362.
Shanmugam, G., 2017. Global case studies of soft-sediment deformation structures (SSDS): definitions, classifications, advances, origins, and problems. Journal of Palaeogeography 6, 251–320.
Catálogo de los efectos geológicos de los terremotos en España. In: Silva, P.G., Rodríguez-Pascua, M.A. (Eds.), IGME, Serie Riesgos Geológicos y Geotecnia. vol. 4 (358 pp.).
Taj, R.J., Aref, M.A.M., Schreiber, B.C., 2014. The influence of microbial mats on the formation of sand volcanoes and mounds in the Red Sea coastal plain, south Jeddah, Saudi Arabia. Sedimentary Geology 311, 60–74.
Törő, B., Pratt, B.R., 2016. Sedimentary record of seismic events in the Eocene Green River Formation and its implications for regional tectonics on lake evolution (Bridger Basin, Wyoming). Sedimentary Geology 344, 175–204.
Toussaint, R., Aharonov, E., Koehn, D., Gratier, J.-P., Ebner, M., Baud, P., Rolland, A., Renard, F., 2018. Stylolites: a review. Journal of Structural Geology 114, 163–195.
Vai, G.B., Ricci-Lucchi, F., 1977. Algal crusts, autochtonous and clastic gypsum in a cannibalistic evaporite basin: a case history from the Messinian of northern Apennines. Sedimentology 24, 211–244.
van Loon, A.J., 2009. Soft-sediment deformation structures in siliciclastic sediments: an overview. Geologos 15, 3–55.
van Loon, A.J., Mazumder, R., De, S., 2016. The response of stromatolites to seismic shocks: tomboliths from the Palaeoproterozoic Chaibasa Formation, E India. Journal of Palaeogeography 5, 381–390.
Warren, J.K., 2016. Evaporites. Springer (1829 pp.).